Journal of the Korean Nuclear Society
Volume 31, Number 6, pp.595~607, December 1999

Calculation of Proton-Induced Reactions on Ti, Fe, Cu and Mo up to 60 MeV for TLA Application

Doohwan Kim, Young-Ouk Lee, and Jonghwa Chang

Korea Atomic Energy Research Institute
150 Dukjin-dong, Yusong-gu, Taejon 305-353, Korea
dookim@lui.kaeri.re.kr

(Received July 5, 1999)

Abstract

The reaction cross-sections of $^{nat}Ti(p,X)^{48}V$, $^{nat}Fe(p,X)^{56}Co$, $^{nat}Cu(p,X)^{65}Zn$ and $^{nat}Mo(p,X)^{96}Tc$ for TLA application are calculated in the frame of the ECIS-GNASH code system up to 60 MeV. The calculated results are compared with the experimental data taken from the EXFOR at the NEA Data Bank. A preliminary calculation with the global optical parameters of Varner *et al.* shows considerable differences from the experimental data at low energy range. The global optical parameters for the imaginary volume potential and the diffuseness of the imaginary potential are adjusted to achieve a better description of the experimental data in the vicinities of peak position below 16 MeV.

Key Words : proton-indnced reaction, TLA application, ECIS-GNASH code

1. Introduction

During the last thirty years, a global nucleon-nucleus optical-model potential has been used for evaluating reaction and differential cross-sections and analyzing-power angular distributions [1-3]. It has parameters that are smooth functions of target atomic mass number and proton number, projectile type and laboratory bombarding energy. The global-model potentials, different from the optical-model potentials whose parameters are obtained by fitting only the elastic and the inelastic scattering data, can be used to predict nucleon-nucleus potentials if elastic scattering data cannot be obtained as for nuclei far from the valley of stability. The data for the most of proton-induced reactions are not enough and ambiguous in reliability except a few elastic scattering data. Though it is difficult to evaluate the above-mentioned activation cross-sections due to lack of the experimental data, it is of considerable significance for an activation analysis.

The accurate evaluation and calculation for the production of radionuclides in charged-particle-induced nuclear reaction are of importance for a number of practical applications, such as the

design and optimization of radionuclide production routes, the monitoring of beam energies and intensities, charged-particle activation analysis, the description of cosmogenic nuclide production processes and the prediction of residual radioactivity levels in accelerator technology.

Thin layer activation (TLA) [4], one of the practical applications, is a technique which has been used since the 1970's. The technique requires that a component surface be labelled with a known depth profile of radioactivity which decays with the emission of γ rays. By monitoring the surface radioactivity, it is possible to measure the loss of surface due to wear, erosion or corrosion. In 1997, IAEA published a report [4] which describes the TLA method and its applications in industry. ^{48}V, ^{56}Co, ^{65}Zn and ^{96}Tc which are useful for TLA application are produced by means of $^{nat}Ti(p,X)^{48}V$, $^{nat}Fe(p,X)^{56}Co$, $^{nat}Cu(p,X)^{65}Zn$ and $^{nat}Mo(p,X)^{96}Tc$. Chang *et al.* [5] have evaluated the production cross-sections of these reactions by fitting the experimental data. In the present work, these proton-induced reaction cross-sections are calculated up to 60 MeV. The theoretical results obtained by means of the ECIS96-GNASH code system are compared with the experimental data taken from EXFOR database at the NEA Data Bank. A preliminary calculation was carried out with the global optical parameters recommended by IAEA in RIPL (Reference Input Parameter Library) [6] and then more calculations are performed by adjusting the optical parameters for the imaginary volume potential and the diffuseness of the imaginary potential, in order to achieve better agreements with the experimental data. The calculated results are compared with the preliminary results as well as the experimental data.

In Section 2, the ECIS96-GNASH code system and features of each code are presented and the used input and the optical potential parameters for the ECIS96-GNASH code are also described. The calculated results are discussed in Section 3 and the conclusions are summarized in Section 4.

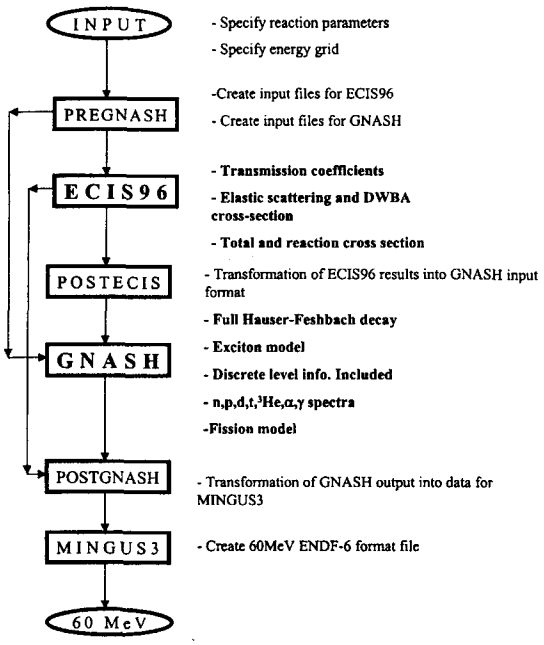

Fig. 1. Flow Chart of the Evaluation Code System

2. Model Calculations

2.1. ECIS96-GNASH Code System

The ECIS96-GNASH code system [7] is used for performing the nuclear model calculations and storing the results in an ENDF6-format. The purpose of the code system is to automatize the creations of their input files that are necessary at various stages of the process and the calculations with several codes successively. Fig. 1 describes the flow chart of the code system used to produce the calculated cross-sections. The steps involved in the code system are ; (a) specifying the reaction parameters, such as the projectile and target type,

the kind of emission particles, the level density parameters, the giant resonance parameters for γ-transition and so on, and energy grid in the INPUT ; (b) setting up the input information for the ECIS96 [8] and the GNASH [9] using the PREGNASH code ; (c) calculating reaction cross-section, elastic scattering, transmission coefficients, and direct inelastic scattering with the ECIS96; (e) transforming the ECIS96 results into GNASH input format using the POSTECIS code ; (d) running GNASH to determine emission cross-sections and the spectra of n, p, d, t, ^{3}He, α, γ using full Hauser-Feshbash decay model and exciton model; (e) transforming the GNASH output into data for MINGUS3 using the POSTGNAHS code ; and finally (f) running MINGUS3, a code that scans the GNASH output, calculates recoil emission spectra for the heavy isotope products, and generates cross-section in an ENDF6-format up to 60 MeV. In the GNASH, the γ-ray transmission coefficients are obtained by the Kopecky-Uhl model [10] and the continuum level densities by Ignatyuk [11].

2.2. Optical Model Calculations

The present evaluations are based mainly on the model calculations using ECIS96-GNASH code system. A calculation through the code system provides a useful way to interpolate and extrapolate to other energies and atomic masses, and enables the evaluated libraries to be generated for all reaction products in a fully consistent way. The optical model calculations are performed with the ECIS96.

The optical model potential used in the present evaluation is as follows:

$$V(r) = -V_V f_V(r) - iW_{wV} f_{wV}(r) + 4ia_{wd} W_{wd} \frac{df_{wd}(r)}{dr} + \frac{\lambda_\pi^2}{r}\left[V_{so}\frac{df_{so}(r)}{dr} + iW_{so}\frac{df_{wso}(r)}{dr}\right]\vec{\sigma}\cdot\vec{l} \quad (1)$$

where λ_π^2 is the square of the pion Compton wavelength, $f_i(r)$ is the form factor of the Woods-Saxon form defined in $f_i(r) = \frac{1}{1+\exp[(r-R_i)/a_i]}$ and Vv, W_{wV}, W_{wd}, V_{so} and W_{so} are the depths of the real volume, the imaginary volume and surface and the real and imaginary spin-orbit potentials respectively. The quantity $\sigma \cdot l$ is the scalar product of the intrinsic and orbital angular momentum operators. The coefficients are adopted from RIPL [6], and the potentials for protons and neutrons are referenced to Varner *et al.* [3].

These forms for the global nucleon-nucleus optical potential are given as follows :

• Real central potential:

$$V_V = V_0 \pm V_t\frac{N-Z}{A} + (E-E_c)V_e, \quad (2a)$$

$$R_V = r_V A^{1/3} + r_V^{(0)}, \quad (2b)$$

$$E_c = \frac{6Ze^2}{5R_c} = \frac{1.73Z}{R_c}(\mathrm{MeV}), \quad \text{for (p, p)}. \quad (2c)$$

where '+' sign is used for proton potential, '-' sign for neutron and Z, N and A are the numbers of protons, neutrons and nucleons in the target nuclide, respectively. E is the energy of the incident proton.

• Coulomb potential radius:

$$R_c = r_c A^{1/3} + r_c^{(0)} = 1.238A^{1/3} + 0.116\ (\mathrm{fm}) \quad (2d)$$

• Spin-orbit potential radius:

$$R_{so} = r_{so} A^{1/3} + r_{so}^{(0)}. \quad (2e)$$

• Imaginary central potential:

$$W_{wV} = W_{i0}\left[1 + \exp\left(\frac{W_{ve0} - (E-E_c)}{W_{vew}}\right)\right]^{-1}, \quad (2f)$$

$$W_{wd} = \left(W_{s0} \pm W_{st}\frac{N-Z}{A}\right)\left[1 + \exp\left(\frac{(E-E_c) - W_{se0}}{W_{sew}}\right)\right]^{-1}, \quad (2g)$$

Table 1. Preliminary Parameters of the Global Nucleon-nucleus Optical Potential (adopted from reference 3.)

Parameter	Value	Parameter	Value
V_0	52.9±0.2MeV	W_{v0}	7.8±0.3MeV
V_1	13.1±0.8MeV	W_{ve0}	35±1MeV
V_e	−0.299±0.004	W_{vew}	16±1MeV
r_V	1.250±0.002fm		
$r_V^{(0)}$	−0.255±0.009fm	W_{s0}	10.0±0.2MeV
a_V	0.690±0.006fm	W_{st}	18±1MeV
		W_{se0}	36±2MeV
r_c	1.24fm	W_{sew}	37±2MeV
$r_c^{(0)}$	0.12fm	W_{so}	0. MeV
V_{so}	5.9±0.1 MeVfm^2		
r_{so}	1.34±0.03fm	r_{wV}, r_{wd}	1.33±0.01fm
$r_{so}^{(0)}$	−1.2±0.1fm	$r_{wV}^{(0)}$, $r_{wd}^{(0)}$	−0.42±0.03fm
a_{so}	0.63±0.02fm	a_{wV}, a_{wd}	0.69±0.01fm

$$R_{wV} = r_{wV} A^{1/3} + r_{wV}^{(0)},$$
$$R_{wd} = r_{wd} A^{1/3} + r_{wd}^{(0)}. \quad \text{(2h)}$$

The global potential parameter-values with uncertainties are given in Table 1.

The purpose of the preliminary calculation is to examine the applicability of the global optical potential parameters. Varner *et al.* found a new parameter set, one of global optical parameters in RIPL, based on data for A=40 to 209, proton energies of 16 to 65 MeV and neutron energies of 10 to 26 MeV using (p,p) and (n,n) scattering from target nuclei in the valley of stability. The results obtained from the preliminary calculation are in good agreement with experimental data in the incident proton energy of above 16 MeV, but, in below 16 MeV, there is a considerable discrepancy between the calculated results and the experimental data. In many cases, one has combined a couple of global optical potentials which are used in specific energy range, and chosen the transition energies between these different potentials to result in a reaction cross section that changes continuously. However, the present work is not to substitute other potential parameters for Varner's in below 16 MeV, but to expand the energy range of Varner's potential by modifying the global optical potential parameters, especially a volume imaginary potential parameter.

Table 1. Adjusted Parameters of the Global Nucleon-nucleus Optical Potential

	RIPL	a_{wd}		a_w	
		proton	neutron	proton	neutron
p+^{48}Ti	0.69	0.59	0.59	0.59	0.59
p+^{56}Fe	0.69	0.51	0.51	0.69	0.69
p+^{65}Cu	0.69	0.59	0.69	0.69	0.69
p+^{96}Mo	0.69	0.69	0.69	0.69	0.69
p+^{97}Mo	0.69	0.65	0.69	0.69	0.69
p+^{98}Mo	0.69	0.65	0.69	0.69	0.69

The imaginary potential is divided into two parts, volume and surface terms. One of the empirical characteristics of the imaginary absorptive potential is the transition from principally surface-dominated absorption at low energies (E<20MeV), to volume-dominated absorption at higher energies (E>60MeV). In most of the optical parameters, the volume imaginary potential is not taken into account below about 16 MeV [1-2]. Also, in the low energy range, since an interaction between incident proton and target nucleus become active in the vicinities of the surface of target nucleus, it is an effective approach to vary the diffuseness of the imaginary potential which is sensitive to the surface effect. The adjusted and RIPL parameters of the global nucleon-nucleus optical potential are shown in Table 2.

Potentials for the other ejectiles are also needed for calculating transmission coefficients for their decay. Potential parameters for global α-particles, deuterons and ^{3}He which are validated for wide mass and energy range are adopted for Avrigeanu *et al.*, Bojowald *et al.* and Becchetti *et al.* [12]

respectively. The same α-particle, deuteron and ^{3}He optical parameters are applied for ^{nat}Ti, ^{nat}Fe, ^{nat}Cu and ^{nat}Mo, since a change of them contributes a little to the proton-induced reactions, especially (p,n) reaction, and current reaction channels do not include the emission of deuteron, triton, ^{3}He and α-particle at low energy.

2.3. ^{nat}Ti(p,X)^{48}V

Natural titanium has five stable isotopes, ^{46}Ti (8.25 %), ^{47}Ti (7.44 %), ^{48}Ti (73.72 %), ^{49}Ti (5.41 %) and ^{50}Ti (5.18 %). To obtain ^{nat}Ti(p,X) ^{48}V, we need to evaluate three reactions of ^{nat}Ti isotopes, which are calculated by the following relation :

$$\sigma\{^{nat}\text{Ti(p,X)}^{48}\text{V}\} = 0.7372 * \sigma\{^{48}\text{Ti(p,n)}^{48}\text{V}\} + 0.0541 * \sigma\{^{49}\text{Ti(p,2n)}^{48}\text{V}\} + 0.0518 * \sigma\{^{50}\text{Ti(p,3n)}^{48}\text{V}\} \quad (4a)$$

The second and third terms are ignored, since the natural abundance ratio of ^{49}Ti and ^{50}Ti are small and those of (p,2n) and (p,3n) reactions, in general, are negligible compared with that of (p,n) reaction. Two production cross-sections of proton-induced reactions, ^{48}Ti(p,n)^{48}V and ^{48}Ti(p,2n)^{47}V, are evaluated in order to justify the calculated results for the activation cross-section of ^{nat}Ti(p,X)^{48}V. Levkovskij [13] and Gadioli [18] measured two activation cross-sections of ^{48}Ti(p,n)^{48}V and ^{48}Ti(p,2n)^{47}V, while other authors have only one activation cross-section. Therefore, in the present work, Levkovskij's results at the low energy region and Gadioli's at high energy are adopted as the reference data for two reactions to keep a consistency in sequential decay reaction channels.

2.4. ^{nat}Fe(p,X)^{56}Co

Natural iron has four stable isotopes, ^{54}Fe (5.845 %), ^{56}Fe (91.754 %), ^{57}Fe (2.119 %) and ^{58}Fe (0.282 %). To obtain ^{nat}Fe(p,X)^{56}Co, we need to evaluate two reactions of ^{nat}Fe isotopes, which are calculated by the following relation :

$$\sigma\{^{nat}\text{Fe(p,X)}^{56}\text{Co}\} = 0.91754 * \sigma\{^{56}\text{Fe(p,n)}^{56}\text{Co}\} + 0.02119 * \sigma\{^{57}\text{Fe(p,2n)}^{56}\text{Co}\}. \quad (4b)$$

The second term for the activation cross-section for ^{57}Fe is ignored, since the natural abundance ratio of ^{57}Fe is very small compared to that of ^{56}Fe. Two production cross-sections of proton-induced reactions, such as ^{56}Fe(p,n)^{56}Co and ^{56}Fe(p,2n)^{55}Co, are evaluated in order to justify the calculated results for the activation cross-section of ^{nat}Fe(p,X)^{56}Co. In the present work, similar to the calculation for ^{nat}Ti(p,X)^{48}V, Levkovskij's results [13] are adopted as reference data for ^{56}Fe(p,n)^{56}Co and ^{56}Fe(p,2n) ^{55}Co.

2.5. ^{nat}Cu(p,X)^{65}Zn

Natural copper has two stable isotopes, ^{63}Cu (69.17 %) and ^{65}Cu (30.83 %). To obtain ^{nat}Cu activation cross-section, we evaluate ^{65}Cu(p,n)^{65}Zn reaction and use the following relation :

$$\sigma\{^{nat}\text{Cu(p,X)}^{65}\text{Zn}\} = 0.3083 * \sigma\{^{65}\text{Cu(p,n)}^{65}\text{Zn}\}. \quad (4c)$$

There are few experimental data for p+^{65}Cu reaction except for ^{65}Cu(p,n)^{65}Zn. Although the experimental data for ^{65}Cu(p,n)^{65}Zn are collected enough, three different data groups shown in Fig. 8 make the evaluation be difficult. In the present work, Michel's [24] and Mills' results [41] are adopted as the reference data for ^{nat}Cu(p,X)^{65}Zn.

2.6. ^{nat}Mo(p,X)^{96}Tc

Natural molybdenum has seven stable isotopes, ^{92}Mo (14.84 %), ^{94}Mo (9.25 %), ^{95}Mo (15.92 %), ^{96}Mo (16.68 %), ^{97}Mo (9.55 %), ^{98}Mo (24.13 %) and ^{100}Mo (9.63 %). In order to obtain ^{nat}Mo

Table 3. The Relevant and Complementary Reaction Cross-sections

Activation cross-sections	Relevant reaction cross-sections	Complementary reaction cross-sections
$^{nat}Ti(p,X)^{48}V$	$^{48}Ti(p,n)^{48}V$	$^{48}Ti(p,2n)^{47}V$
$^{nat}Fe(p,X)^{56}Co$	$^{56}Fe(p,n)^{56}Co$	$^{56}Fe(p,2n)^{55}Co$
$^{nat}Cu(p,X)^{65}Zn$	$^{65}Cu(p,n)^{65}Zn$	
$^{nat}Mo(p,X)^{96}Tc$	$^{96}Mo(p,n)^{96}Tc$	$^{96}Mo(p,2n)^{95}Tc$
	$^{97}Mo(p,2n)^{96}Tc$	$^{97}Mo(p,3n)^{95}Tc$
	$^{98}Mo(p,3n)^{96}Tc$	$^{98}Mo(p,n)^{98}Tc$

activation cross-section, we need to evaluate four reactions of ^{nat}Mo isotopes, which are added up by the following relation :

$$\sigma\{^{nat}Mo(p,X)^{96}Tc\} = 0.1668 * \sigma^{96}\{Mo(p,n)^{96}Tc\} + 0.0955 * \sigma\{^{97}Mo(p,2n)^{96}Tc\} + 0.2413 * \sigma\{^{98}Mo(p,3n)^{96}Tc\} + 0.0963 * \sigma\{^{100}Mo(p,5n)^{96}Tc\}. \quad (4d)$$

The fourth term is ignored, since (p,5n) reaction is difficult to take place. Since there exist no experimental data for $^{nat}Mo(p,X)^{96}Tc$, the calculated results for the activation cross-section of $^{nat}Mo(p,X)^{96}Tc$ are justified by evaluating the several activation cross-sections; $^{96}Mo(p,n)^{96}Tc$, $^{96}Mo(p,2n)^{95}Tc$, $^{97}Mo(p,2n)^{96}Tc$, $^{97}Mo(p,3n)^{95}Tc$, $^{98}Mo(p,n)^{98}Tc$ and $^{98}Mo(p,3n)^{96}Tc$. Levkovskij [13] measured five activation cross-sections ; $^{96}Mo(p,n)$, $^{97}Mo(p,2n)$, $^{98}Mo(p,3n)^{96}Tc$, and $^{96}Mo(p,2n)$, $^{97}Mo(p,3n)^{95}Tc$. In the present evaluation, Levkovskij's results are adopted as reference data to keep a consistency in sequential decay reaction channels.

3. Results and Discussion

Evaluating the activation cross-sections of $^{nat}Ti(p,X)^{48}V$, $^{nat}Fe(p,X)^{56}Co$, $^{nat}Cu(p,X)^{65}Zn$ and $^{nat}Mo(p,X)^{96}Tc$, we should calculate the relevant and complementary reaction cross-sections listed in Table 3. 'RIPL' in the figures 2~15 indicate

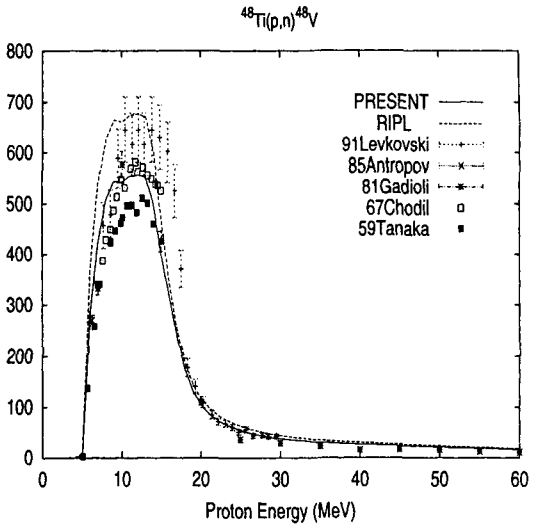

Fig. 2. Production Cross Section on $^{48}Ti(p,n)^{48}V$

the calculated results obtained from the preliminary calculation. Though the preliminary calculation gives reasonable results, more accurate evaluations need to be performed by adjusting the global optical parameters to achieve a better description of the experimental data. 'PRESENT' in the figures 2~16 indicate the evaluated results from the present work.

3.1. Calculated Results for $^{nat}Ti(p,X)^{48}V$

Figures 2, 3 and 4 show the present results together with the preliminary calculated results and the experimental data. There are considerable discrepancies between the preliminary calculation for $^{48}Ti(p,n)^{48}V$ and $^{nat}Ti(p,X)^{48}V$ indicated as 'RIPL', and the experimental data. The calculated results for $^{48}Ti(p,2n)^{47}V$ and $^{nat}Ti(p,X)^{48}V$ are in good agreement with the experimental data, while that for $^{48}Ti(p,n)^{48}V$ is lower than the experimental data. However, as shown in Eq. (4a), the calculation can not reproduce the corresponding experimental data, $^{48}Ti(p,n)^{48}V$ and $^{nat}Ti(p,X)^{48}V$, simultaneously. In the present work, $^{nat}Ti(p,X)^{48}V$ are chosen as reference data.

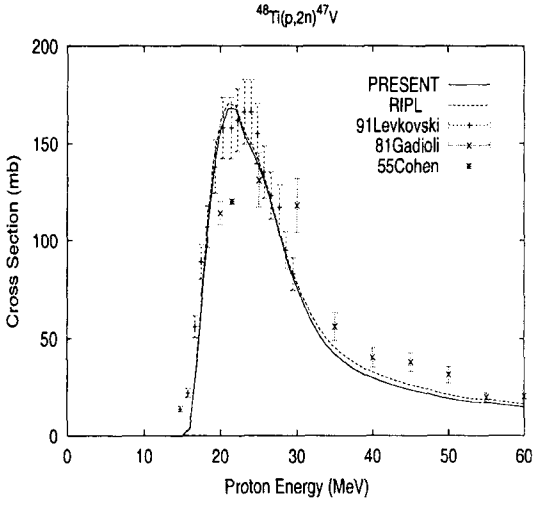

Fig. 3. Production Cross Section on ^{48}Ti(p,2n)^{47}V

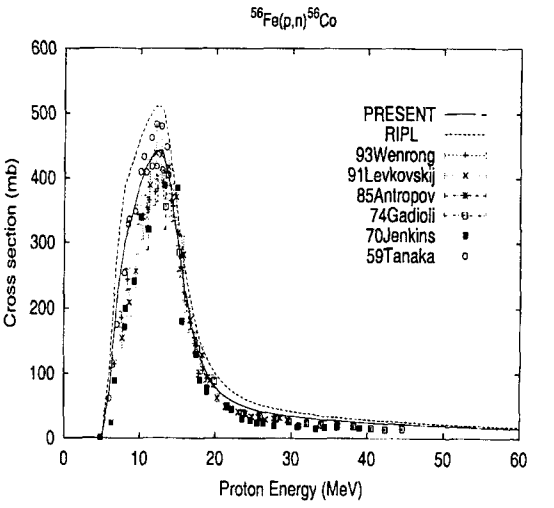

Fig. 5. Production Cross Section on ^{56}Fe(p,n)^{56}Co

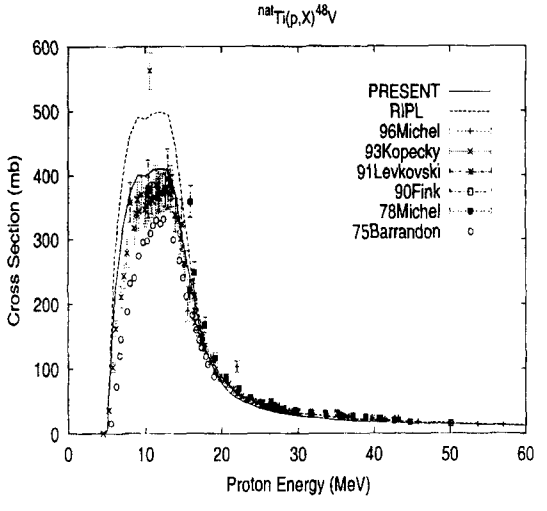

Fig. 4. Production Cross Section on ^{nat}Ti(p,X)^{48}V

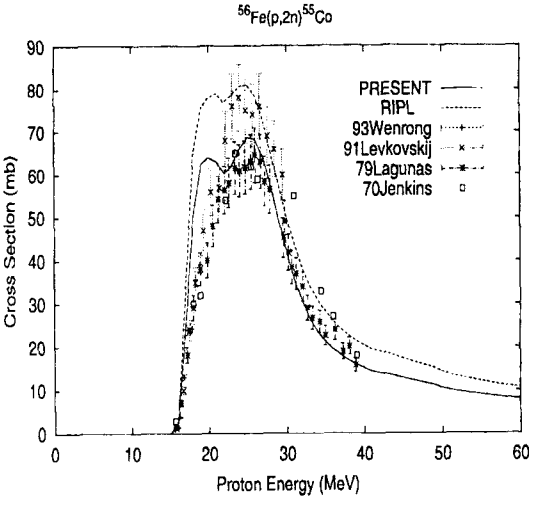

Fig. 6. Production Cross Section on ^{56}Fe(p,2n)^{55}Co

3.2. Calculated Results for ^{nat}Fe(p,X)^{56}Co

Figures 5 and 7 show that the results of the present evaluation for ^{56}Fe(p,n)^{56}Co and ^{nat}Fe(p,X)^{56}Co are in good agreement with the experimental data, while Fig. 6 for ^{56}Fe(p,2n)^{55}Co shows a two-peaks which is not appeared in experimental data. So, we choose to evaluate the cross-section for ^{56}Fe(p,2n)^{55}Co which is higher than the experimental data below 22 MeV and lower than above 22 MeV. Nevertheless the calculated results for ^{nat}Fe(p,X)^{56}Co reproduce well the experimental data of Takacs' [14].

3.3. Calculated Results for ^{nat}Cu(p,X)^{65}Zn

Figure 8 shows four groups of the experimental data for ^{65}Cu(p,n)^{65}Zn. The

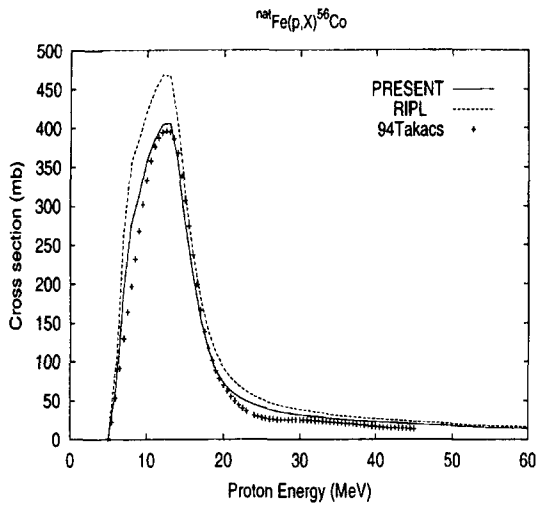

Fig. 7. Production Cross Section on $^{nat}Fe(p,X)^{56}Co$

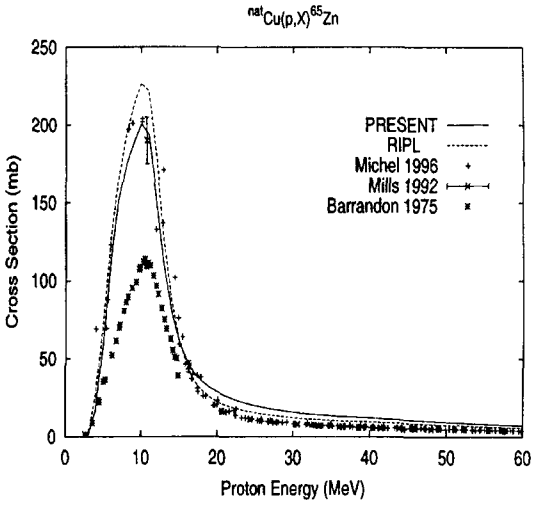

Fig. 9. Production Cross Section on $^{nat}Cu(p,X)^{65}Zn$

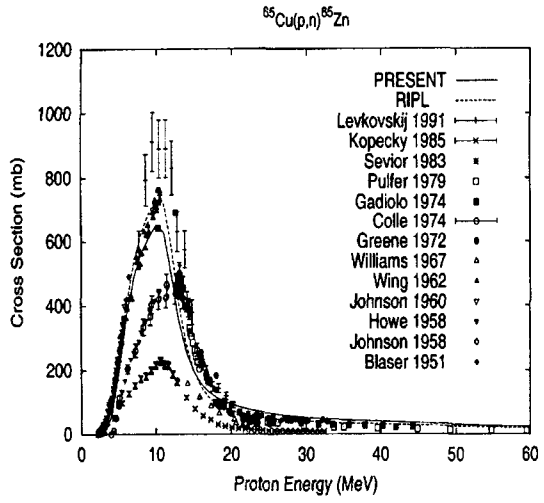

Fig. 8. Production Cross Section on $^{65}Cu(p,n)^{65}Zn$

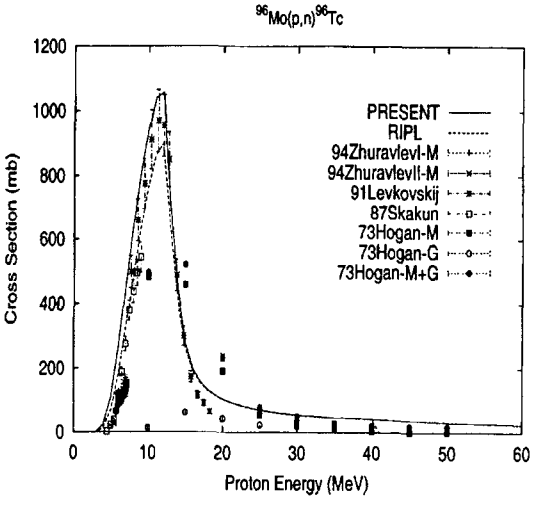

Fig. 10. Production Cross Section on $^{96}Mo(p,n)^{96}Tc$

experimental data for $^{nat}Cu(p,X)^{65}Zn$ are reproduced first by adopting those of Michel [24] and Mills [41] as the reference data, and are in good agreement with the calculated results shown in Fig. 9. By the simple algebraic relation given in Eq. (4c), the cross-sections for $^{65}Cu(p,n)^{65}Zn$ can be obtained easily from those for $^{nat}Cu(p,X)^{65}Zn$. The calculated results for $^{65}Cu(p,n)^{65}Zn$ reproduce well the experimental data above 15 MeV except for those of Kopecky *et al.* [30] and Williams *et al.* [35]

3.4. Calculated Results for $^{nat}Mo(p,X)^{96}Tc$

To evaluate the production cross-section for $^{nat}Mo(p,X)^{96}Tc$, the activation cross-section data for $^{96}Mo(p,n)^{96}Tc$, $^{97}Mo(p,2n)^{96}Tc$ and $^{98}Mo(p,3n)^{96}Tc$ need to be calculated. The calculated results for

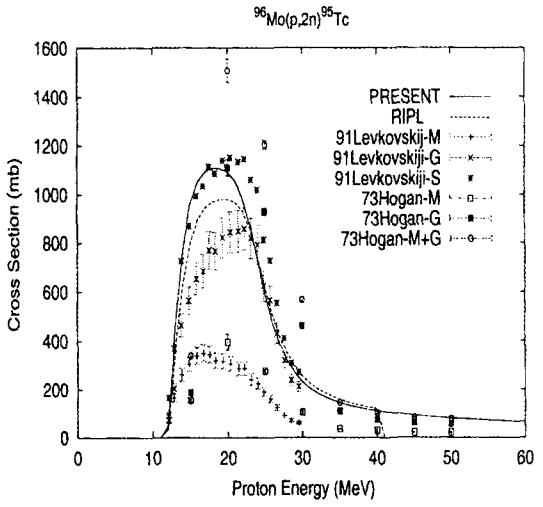

Fig. 11. Production Cross Section on ^{96}Mo(p,2n) ^{95}Tc

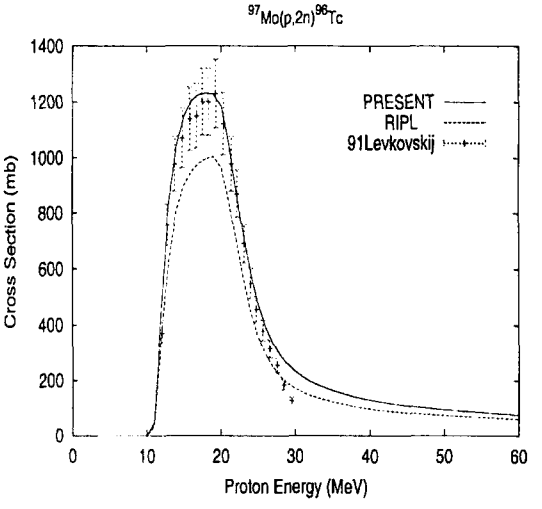

Fig. 12. Production Cross Section on ^{97}Mo(p,2n) ^{96}Tc

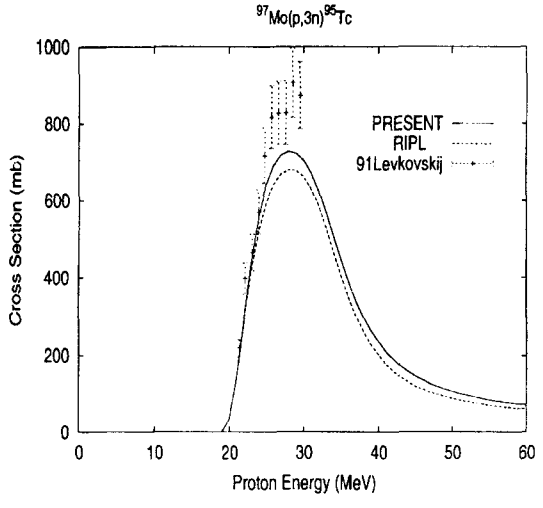

Fig. 13. Production Cross Section on ^{97}Mo(p,3n) ^{95}Tc

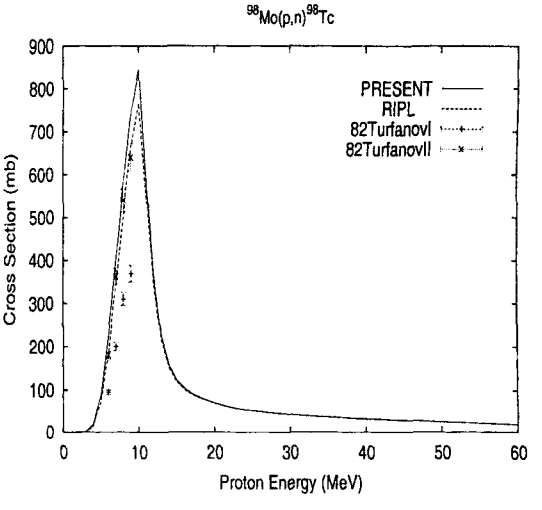

Fig. 14. Production Cross Section on ^{98}Mo(p,n) ^{98}Tc

^{96}Mo(p,n)^{96}Tc, ^{97}Mo(p,2n)^{96}Tc and ^{98}Mo(p,3n)^{96}Tc are in good agreement with the experimental data as shown in Fig. 10, 12 and 14, respectively. Therefore, in Fig. 16, the values obtained through the simple relation in Eq. (4d) are reliable though no experimental data exist. 'M', 'G' and 'M+G' in the figures indicate the experimental data for meta-stable state, ground state and the all states of the remained nucleus, respectively. 'S' indicates the sum of cross-sections for two states, meta-stable and ground state, taken from the experimental data.

4. Conclusions

We have evaluated proton-induced nuclear

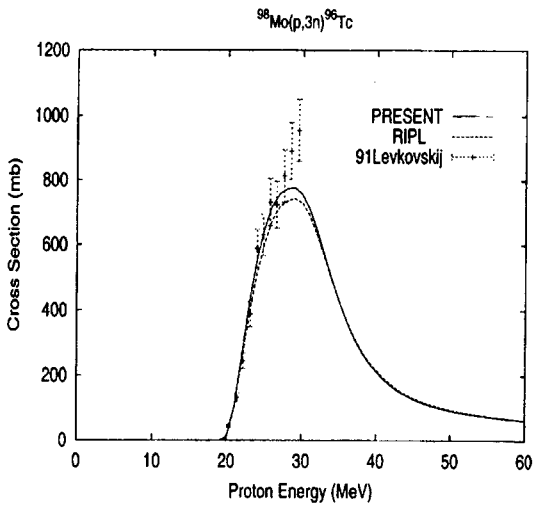

Fig. 15. Production Cross Section on ^{98}Mo(p,3n) ^{96}Tc

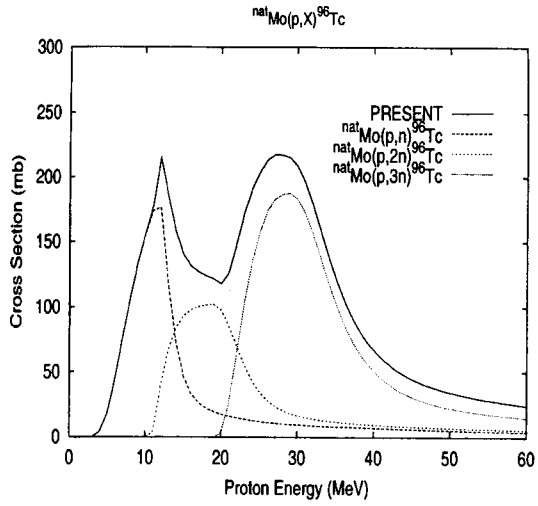

Fig. 16. Production Cross Section on ^{nat}Mo(p,X) ^{96}Tc

data of ^{nat,48}Ti, ^{nat,56}Fe, ^{nat,65}Cu and ^{nat,96,97,98}Mo up to 60 MeV by ECIS-GNASH code system. The present work is to expand the energy range of Varner's potential within proton energies of 16 MeV to 65 MeV and neutron energies of 10 to 26 MeV by modifying the optical potential parameters, especially the volume imaginary potential parameter and the diffuseness of the imaginary potential. The calculated results are in agreement with the measured data, which means that the adopted neutron and proton global optical potential parameters are appropriate for calculation of transmission coefficients needed in the statistical model based on the Hauser-Feshbach formalism.

Acknowledgement

This work was performed under the auspices of Korea Ministry of Science and Technology as one of long-term nuclear R&D programs.

References

1. D. Becchetti and G.W.Greenlees, "Nucleon-Nucleus Optical-Model Parameters, A>40, E<50 MeV", *Phys. Rev.* **182**, 1190 (1969).
2. J. Raport, V. Kulkarni and R.W. Finlay, "A Global Optical-Model Analysis of Neutron Elastic Scattering Data", *Nucl. Phys.* **A330**, 15 (1979).
3. R.L. Varner, W.J. Thompson, T.L. McAbee, E.J. Ludwig and T.B. Clegg, "A Global Nucleon Optical Model Potential", *Phys. Rep.* **201**, 57-119 (1991).
4. "The thin layer activation method and its applications in industry", *IAEA-TECDOC-***924**, IAEA (1997).
5. J. Chang, S.Y. Oh and J.H. Jin, "Evaluation of Proton Reaction Cross Sections of Major Elements in Metal Substances for Thin Layer Activation Method" in " Proceedings of the of the Korean nuclear Society Autumn Meeting",

30-31 October (1998).

6. P. G. Young, "4. Optical Model Parameters : Handbook for calculations of nuclear reaction data Reference input parameter library", IAEA-TECDOC-1034, August (1998). (WWW-address:http://www-nds.iaea.or.at/ripl)
7. M.B. Chadwick *et al.*, "Cross-Section Evaluations to 150 MeV for Accelerator-Driven Systems and Implementation in MCNPX", *Nucl. Sci. Eng.* **131**, 293-328 (1999).
8. J. Raynal, "Notes on ECIS94", Note CEAN-2772 (1994). ; "ECIS94" in "Proceedings of a Specialists Meeting on the Nucleon-Nucleus Optical Model up to 200 MeV", 13-15 November, Bruyeres-Chatel, France (1996).
9. P.G. Young, E.D. Arthur and M.B. Chadwick, "Comprehensive Nuclear Model Calculations : Introduction to the Theory and Use of the GNASH Code", in "Workshop on Computation and Analysis of Nuclear data Relevant to Nuclear Energy and Safety", 10 February- 13 March, Trieste, Italy (1992).
10. J. Kopecky and M. Uhl, "Test of γ-Ray Strength Functions in Nuclear-Reaction Model-Calculations", *Phys. Rev.* ***C42***, 1941 (1990).
11. A.V. Ignatyuk, G.N. Smirenkin, and A.S. Tishin, "Phenomenological Description of the Energy Dependence of the Level Density Parameter", *Sov. J. Nucl. Phys.* **21**, 255 (1975).
12. J. Kopecky, "5. γ-Ray Strength Functions : Handbook for calculations of nuclear reaction data Reference input parameter library", *IAEA-TECDOC*-1034, August 1998. (WWW-address:http://www-nds.iaea.or.at/ripl).
13. V.N. Levkovskij, "Activation Cross Section Nuclides of Average Masses (A=40-100) by Protons and α-Particles with Average Energies (E=10-50 MeV)", (1991), EXFOR entry A0510.
14. S. Takacs, L. Vasvary and F. Tarkanyi, "Remeasurement and Compilation of Excitation Function of Proton Induced Reactions on Iron for Activation Techniques", *Nucl. Inst. Method* **B89**, 88 (1994), EXFOR entry D4026.
15. R. Michelit *et al.*, "Cross Sections for the Production of Residual Nuclides by Low- and Medium-Energy Protons from the Target Elements C, N. O. Mg, Al, Si, Ca, Ti, V, Mn, Fe, Co, Ni, Cu, Sr, Y, Zr, Nb, Ba and Au", *Nucl. Inst. Method* **B127**, 153 (1996), EXFOR entry O0276.
16. A.M. Trufanov *et al.*,*Yad. Fizika* **36**, 299 (1982), EXFOR entry A0164.
17. A.E. Antropovit *et al.*, "Cross Sections Measurements of (p,n), (α,pn), (α,xn) Reactions on Nuclei Middle Atomic Weight", (1985), EXFOR entry O0076.
18. E. Gadioliit *et al.*, "Emission of α Particles in the Interaction of 10-85 MeV Protons with Ti-48,50", *Z. Phys.* **A301**, 289 (1981), EXFOR entry D4060.
19. G. Chodil, *Nucl. Phys.* **93**, 648 (1967), EXFOR entry P0021.
20. S. Tanaka, "Excitation Functions for (p,X) Reactions with Titanium, Vanadium, Chromium, Iron and Nickel up to 14 MeV", *J. of the Phys. Soc. Japan* **14**, 1269 (1959), EXFOR entry B0043.
21. B.L. Cohen, E. Newman, "(p,pn) and (p,2n) Cross Sections in Medium Weight Elements", *Phys. Rev.* **99**, 718 (1955), EXFOR entry B0050.
22. P. Kopecky *et al.*,"Excitation Functions of (p,xn) Reactions on Nat-Ti : Monitoring of Bombarding Proton Beams", *Appl. Radiation and Isotopes* **44**, 687 (1993), EXFOR entry D4001.
23. D. Fink *et al.*, "Production of 41Ca and K, Sc and V Short-Lived Isotopes by the Irradiation

of Ti with 35 to 150 MeV Protons : Applications to Solar Cosmic Ray Studies", *Nucl. Inst. Method* **B52**, 601 (1990), EXFOR entry C0430.

24. R. Michel *et al.*, "Proton-Induced Reactions on Titanium with Energies between 13 and 45 MeV", *J. of Inorganic and Nucl.* Chemistry **40**, 1845 (1978), EXFOR entry B0100.
25. J.N. Barrandon *et al.*, "A Study of the Main Radioisotopes Obtained by Irradiation of Ti, V, Cr, Fe, Ni, Cu and Zn with Protons from 0 to 20 MeV", *Nucl. Inst. and Method* **127**, 269 (1975), EXFOR entry O0086.
26. Z. Wenrong, L. Hanlin, Y. Weixiang, "Measurement of Cross Sections by Bombarding Fe with Protons up to 19 MeV", *Chin. J. Nucl. Phys.* **15**, 337 (1993), EXFOR entry S0041.
27. E. Gadioli *et al.*, "Excitation Functions of V-51, Fe-56, Cu-65 (p,X) Reactions between 10 and 45 MeV", *Nuove Cimento* **A22**, 547 (1974), EXFOR entry B0027.
28. I.L. Jenkins, "Excitation Functions for the Bombardment of Fe-56 with Protons", *J. of Inorganic and Nucl. Chemistry* **32**, 1419 (1970), EXFOR entry B0041.
29. M.C. Lagunas-Solarit *et al.*, *Appl. Radiation and Isotopes* **30**, 25 (1979), EXFOR entry A0182.
30. P. Kopecky, "Proton Beam Monitoring via the Cu(p,X)Co-58, Cu-63(p,2n)Zn-62, Cu-65(p,n)Zn-65 Reactions in Copper", *Appl. Radiation and Isotopes* **36**, 657 (1985), EXFOR entry A0333.
31. M.E. Sevior *et al.*, "Absolute Cross Sections of Proton Induced Reactions on Cu-65, Ni-64, Cu-63", *Aust. Jour. of Physics* **36**, 463 (1983), EXFOR entry A0198.
32. P. Pulfer, "Determination of Absolute Production Cross Sections for Proton Induced Reactions in the Energy Range 15 to 72 MeV and at 1820 MeV", (1979), EXFOR entry D0053. 33. R. Colle *et al.*, "Excitation Functions for (p,n) Reactions to 25 MeV on Cu-63, Cu-65 and Ag-107", *Phys. Rev.* **C9**, 1819 (1974), EXFOR entry B0057.
34. M.W. Greene and E. Lebowitz, "Proton Reactions with Copper for Auxiliary Cyclotron Beam Monitoring", *Appl. Radiation and Isotopes* **23**, 342 (1972), EXFOR entry B0074.
35. I.R. Williams and C.B. Fulmer, "Excitation Functions for Radioactive Isotopes Produced by Protons below 60 MeV on Al, Fe and Cu", *Phys. Rev.* **162**, 1055 (1967), EXFOR entry B0073.
36. J. Wing and J.R. Huizenga, "(p,n) Cross Sections of V-51, Cr-52, Cu-63, Cu-65, Ag-107, Ag-109, Cd-111, Cd-114 and La-139 from 5 to 10.5 MeV", *Phys. Rev.* **128**, 280 (1962), EXFOR entry B0065.
37. C.H. Johnson, A. Galonsky, C.N. Inskeep, "Cross Sections for (p,n) Reactions in Intermediate-Weight Nuclei", *ORNL-***2910** (1960), EXFOR entry B0068.
38. H.A. Howe, "(p,n) Cross Sections of Copper and Zinc", *Phys. Rev.* **109**, 2083 (1958), EXFOR entry B0060.
39. C.H. Johnson *et al.*, "Proton Strength Functions from (p,n) Cross Sections", *Phys. Rev.* **109**, 1243 (1958), EXFOR entry B0046.
40. J.P. Blaser *et al.*, "Fonctions d'Excitation de la Reaction (p,n), I", *Helvetica Physica Acta* **24**, 3 (1951), EXFOR entry B0048.
41. I.R. Mills, G.F. Steyn and F.M. Nortier, "Experimental and Theoretical Excitation Functions of Radionuclides Produced in Proton Bombardment of Copper up to 200 MeV", *Appl. Radiation and Isotopes* **43**, 1019 (1992), EXFOR entry A0507.
42. Y.Y. Zhuravlev *et al.*, *Izv. Akad. Nauk Sssr,*

Ser. Fiz. **58**(5), 106 (1995), EXFOR entry A0575.

43. E.A. Skakun *et al.*,"Excitation Functions and Isomer Ratios for up to 9 MeV Proton Interactions with Zr and Mo Isotope Nuclei." *Yad. Fizika* **46(1)**, 28 (1987), EXFOR entry A0338.
44. J.J. Hogan, "Mo-96 (p,xn) Reaction from 10 to 80 MeV", *Phys. Rev.* **C6**, 810 (1972), EXFOR entry B0025.